Am J Physiol Lung Cell Mol Physiol 288: L1179–L1192, 2005.
First published January 28, 2005; doi:10.1152/ajplung.00450.2004.

Keratinocyte growth factor therapy in murine oleic acid-induced acute lung injury

K. Ulrich,[1] M. Stern,[1] M. E. Goddard,[2] J. Williams,[1] J. Zhu,[1] A. Dewar,[3] H. A. Painter,[4] P. K. Jeffery,[1] D. R. Gill,[4] S. C. Hyde,[4] D. M. Geddes,[1] M. Takata,[2] and E. W. F. W. Alton[1]

[1]*Department of Gene Therapy, National Heart and Lung Institute, and* [2]*Anaesthetics and Intensive Care, Chelsea and Westminster Hospital, and* [3]*Electron Microscopy Unit, National Heart and Lung Institute, Faculty of Medicine, Imperial College London, London; and* [4]*Gene Medicine Research Group, Nuffield Department of Clinical Laboratory Sciences, University of Oxford, United Kingdom*

Submitted 1 December 2004; accepted in final form 24 January 2005

Ulrich, K., M. Stern, M. E. Goddard, J. Williams, J. Zhu, A. Dewar, H. A. Painter, P. K. Jeffery, D. R. Gill, S. C. Hyde, D. M. Geddes, M. Takata, and E. W. F. W. Alton. Keratinocyte growth factor therapy in murine oleic acid-induced acute lung injury. *Am J Physiol Lung Cell Mol Physiol* 288: L1179–L1192, 2005. First published January 28, 2005; doi:10.1152/ajplung.00450.2004.—Alveolar type II (ATII) cell proliferation and differentiation are important mechanisms in repair following injury to the alveolar epithelium. KGF is a potent ATII cell mitogen, which has been demonstrated to be protective in a number of animal models of lung injury. We have assessed the effect of recombinant human KGF (rhKGF) and liposome-mediated KGF gene delivery in vivo and evaluated the potential of KGF as a therapy for acute lung injury in mice. rhKGF was administered intratracheally in male BALB/c mice to assess dose response and time course of proliferation. SP-B immunohistochemistry demonstrated significant increases in ATII cell numbers at all rhKGF doses compared with control animals and peaked 2 days following administration of 10 mg/kg rhKGF. Protein therapy in general is very expensive, and gene therapy has been suggested as a cheaper alternative for many protein replacement therapies. We evaluated the effect of topical and systemic liposome-mediated KGF-gene delivery on ATII cell proliferation. SP-B immunohistochemistry showed only modest increases in ATII cell numbers following gene delivery, and these approaches were therefore not believed to be capable of reaching therapeutic levels. The effect of rhKGF was evaluated in a murine model of OA-induced lung injury. This model was found to be associated with significant alveolar damage leading to severe impairment of gas exchange and lung compliance. Pretreatment with rhKGF 2 days before intravenous OA challenge resulted in significant improvements in P_{O_2}, P_{CO_2}, and lung compliance. This study suggests the feasibility of KGF as a therapy for acute lung injury.

acute respiratory distress syndrome; alveolar epithelial damage; oleic acid; gene therapy

ARDS (acute respiratory distress syndrome) is a term generally applied to patients with severe manifestations of acute lung injury (ALI) and is characterized by severe alveolar damage. In histopathological terms, this encompasses capillary congestion, interstitial and alveolar edema, hyaline membrane formation, and alveolar type I (ATI) cell necrosis (4). ATI cells are large, with volumes of ~3,000 μm^3/cell, and each cell forms a thin (~0.2 μm) cytoplasmic sheet (51) to facilitate gas exchange, which extends from the nucleus to cover the surface of one or more alveoli. Related to both this morphology and their inability to undergo mitosis and cellular repair, ATI cells are particularly sensitive to damage by injurious agents. The alveolar type II (ATII) cell is cuboidal and contains numerous cytoplasmic organelles, including lamellar bodies, for the cytoplasmic production and storage of surfactant (27). Importantly, the ATII cell is critical to the repair process following alveolar epithelial injury and has been shown to be involved in a combination of proliferation and differentiation (1), migration (30, 76), and spreading (30) to cover areas of denuded alveolar epithelium. Thus ATII cell proliferation is believed to be particularly important during repair, as ATII cells differentiate into ATI cells, and thus replace ATI cells lost during the injury phase.

Human keratinocyte growth factor (KGF) was first cloned in 1989 from an embryonic fibroblast cell line by Finch et al. (19). KGF is a heparin-binding growth factor that is secreted by fibroblasts and is known to act via a receptor specific to epithelial cells (37). KGF induces potent proliferative activity in a variety of epithelial cells including keratinocytes, important to hair follicle development (8) and skin growth during wound healing (35). Additionally, KGF stimulates proliferation of mammary (62) and pancreatic ductal epithelia (75). Importantly, KGF also stimulates proliferation of ATII cells in vitro (47) and in vivo (18). Intratracheal administration of recombinant human KGF (rhKGF) to normal rat lungs results in ATII cell hyperplasia 2 days following administration (63). This process initially produces a "piled up" appearance to the alveolar epithelium, caused by the increased number of ATII cells. By *day 3*, however, the newly formed ATII cells appear to migrate outward to cover a larger area of the alveoli, and by *day 6*, the alveolar epithelium appears normal. However, not all newly formed ATII cells differentiate into ATI cells, and apoptosis has been shown to be involved in maintaining homeostasis between cell populations in the lung (18, 57).

Administration of exogenous rhKGF has been shown to ameliorate lung injury in a range of animal models. A number of studies have demonstrated that KGF pretreatment resulted in reduced mortality following intratracheal instillation of hydrochloric acid (43, 71), intratracheal bleomycin (55, 73), hyperoxia (5, 46) and *Pseudomonas aeruginosa*-induced lung injury (65). Amelioration of both morphological damage to the alveolar epithelium and inflammation has been demonstrated in the bleomycin (22) and hydrochloric acid models (43, 71), *P. aeruginosa*-induced lung injury (65), and hyperoxia-induced lung injury (5, 46). Exogenous KGF upregulates active ion transport by increasing the expression of sodium pumps, pri-

Address for reprint requests and other correspondence: Prof. E. W. F. W. Alton, Dept. of Gene Therapy, National Heart and Lung Institute, Manresa Road, London SW3 6LR, United Kingdom (E-mail: e.alton@ic.ac.uk).

The costs of publication of this article were defrayed in part by the payment of page charges. The article must therefore be hereby marked "*advertisement*" in accordance with 18 U.S.C. Section 1734 solely to indicate this fact.

marily the Na^+-K^+-ATPase α_1-subunit (6). Thus in the α-naphthylthiourea model of acute permeability edema, KGF administration reduced lung wet-to-dry weight ratios and bronchoalveolar lavage (BAL) protein (21, 36). Both of these effects were also demonstrated in *P. aeruginosa*-induced (65) and ventilator-induced lung injury (67).

The protective effects of KGF observed in the above studies suggest that, in addition to ATII cell hyperplasia, KGF may have many other beneficial effects on ALI. These may include scavenging of reactive oxygen species and increased DNA repair (59, 69). Additionally, KGF has been implicated in the reduction of alveolar epithelial susceptibility to mechanical deformation in vitro (44), possibly related to changes in the cytoskeleton or the extracellular matrix. Furthermore, KGF accelerates the rate of wound closure during mechanical deformation in various cell lines and primary cells by a combination of increased cell migration rate and cell spreading (20, 66). Atabai et al. (2) demonstrated that KGF-treated cells were more adherent to the extracellular matrix. Enhanced epithelial cell adherence to the denuded basement membrane may provide more rapid restoration of the alveolar architecture following lung injury (49). KGF also directly affects the expression of surfactant (70) and has been shown to stimulate the synthesis of all surfactant components in rat fetal ATII cells, thereby promoting maturation of the lung epithelium (7).

These studies raise the possibility that exogenous recombinant KGF protein might be used to stimulate alveolar epithelial repair in ALI and thus become a future therapy for ARDS. However, the significant cost of large quantities of rhKGF would likely limit the possibilities of prophylactic studies, particularly in larger animals and humans. Gene therapy, in which transfer of *KGF* DNA to alveolar epithelial cells may result in prolonged protein expression, has been proposed as an alternative approach. Thus, topical or systemic application of KGF-encoding plasmid DNA, complexed with cationic liposomes, may result in sufficient expression to produce ATII cell proliferation. Recently, the feasibility of this approach was demonstrated by Jeschke et al. (28) using liposome-mediated *KGF* gene transfer to improve dermal and epidermal regeneration following thermal injury in rats.

Several experimental models of lung injury have been developed that demonstrate pathophysiological changes similar to those in ARDS (50). ALI induced by intravenous administration of oleic acid (OA) resembles ARDS in many morphological, histological, and physiological respects (reviewed in Ref. 53). OA-induced lung injury has been studied in many laboratory animal species and is consistently associated with severe respiratory distress characterized by hypoxemia and reduced lung compliance due to acute alveolar damage, intraalveolar hemorrhage, and leakage of proteinaceous fluid into the air spaces (10, 58). Histological changes include intraalveolar edema and hemorrhage, epithelial disruption, fibrin deposition, and formation of hyaline membranes (11, 29, 52). The model has, however, not been well characterized in mice. Gene therapy for ARDS remains a relatively unexplored possibility, and mice have been used extensively as models of gene transfer to the lungs. With a view to investigating the potential of KGF gene therapy for ARDS, we therefore characterized a murine model of OA-induced lung injury and subsequently assessed the potential of both recombinant KGF protein and liposome-mediated gene transfer to ameliorate alveolar damage. For the latter, we assessed both topical and systemic administration, since KGF is a secreted protein, which may produce its biological effects whether produced by alveolar epithelium or pulmonary endothelium.

MATERIALS AND METHODS

Plasmid DNA

The human *KGF* (hKGF) cDNA was kindly supplied by Stuart Aaronson (Derald H. Ruttenberg Cancer Center, Mount Sinai School of Medicine, New York, NY) as a 2.1-kb insert in a pCEV9 backbone. The hKGF insert was excised from the pCEV9 backbone by restriction enzyme digestion and ligated into the eukaryotic expression vector pCI (Promega). The resulting plasmid was termed pCIhKGF. Evaluation of in vivo transfection efficiency was carried out using a plasmid expressing the reporter gene chloramphenicol acetyltransferase (pCF1CAT), kindly supplied by Genzyme (Framingham, MA). Large-scale purification of plasmid DNA for in vivo gene transfer was carried out using Qiagen EndoFree Giga plasmid purification columns according to the manufacturer's recommendations (Qiagen, Crawley, UK).

Intratracheal Administration of rhKGF

Experiments were carried out under the guidelines of the Animals (Scientific procedures) Act 1986, United Kingdom. Male BALB/c mice (6–8 wk, 19–25 g, Harlan) were anesthetized with Hypnorm/Midazolam/water (Hypnorm:MZ:H_2O; 1:1:3, 0.1 ml/10 g body wt). The trachea was visualized by blunt dissection and KGF (Amgen, Thousand Oaks, CA), and 1, 5, 10, or 15 mg/kg body wt was injected directly into the trachea in a volume of no more than 60 μl. Control animals received an equal volume of KGF reconstitution solution (sterile H_2O, 0.0055% Tween 20, Amgen). The incision was closed with two sutures using 6/0 silk braided suture (Johnson & Johnson, Edinburgh, UK), and the animals were left in a heated cage at 30°C until they fully recovered from the anesthetic. Analgesic (Vetagesic, 1 in 100 dilution, 6 μl/g body wt) was administered before surgery.

Immunohistochemical Quantification of ATII Cell Proliferation

At appropriate time points (24 h to 1 wk) following rhKGF administration, animals were killed by dorsal arteriosection under terminal anesthesia, the trachea was cannulated, and the lungs expanded with 800–900 μl of 10% formalin (Sigma, Poole, UK). The lungs were removed in toto, immersed in 10% formalin, fixed overnight at room temperature, processed, and embedded in paraffin wax. Serial 4- to 5-μm sections were cut, and the first section was stained with Harris's hematoxylin and eosin (BDH, Lutterworth, UK) for overall morphology. ATII cells were stained with a rabbit anti-sheep surfactant protein B (SP-B) polyclonal antibody (Chemicon International, Southampton, UK). The SP-B antibody binds to the surfactant producing lamellar bodies within the ATII cell, which following binding to a secondary detection antibody can be visualized as a characteristic brown stain. The antibody also stains SP-B within Clara cells in the airways and any SP-B that has been engulfed by alveolar macrophages. However, airways were not included in the quantification process, and alveolar macrophages are morphologically and spatially distinct from ATII cells. Cross-reactivity was therefore not a confounding problem. Briefly, paraffin-embedded sections were dewaxed, and endogenous peroxidase activity was blocked with 3% H_2O_2. This was followed by 2-h incubation with normal goat serum (DAKO, Ely, UK). Primary antibody binding [rabbit anti-sheep SP-B (Chemicon)] was carried out for 1.5 days at 4°C, followed by binding of biotinylated goat anti-rabbit IgG secondary antibody for 1 h, incubation with streptavidin-horseradish peroxidase (DAKO) for 1 h, and incubation in 3,3′-diaminobenzidine tetrahydrochloride (DAKO) for 15 min. The slides were counterstained in Mayer's hematoxylin

(BDH) for 1–2 min and then washed, dehydrated in graded alcohol, and mounted with DPX mountant (BDH). Immunoreactive ATII cells were identified as cells with brown staining within the cytoplasm and quantified by counting 10 randomly selected fields of view per slide (×200, 1 slide/animal). All slides were evaluated in a blinded fashion.

Topical Gene Transfer

Preparation of lipid67/KGF pDNA complexes. The cationic liposome GL67 (Genzyme) was rehydrated in sterile endotoxin-free water to a final concentration of 1.2 mM. Plasmid DNA was resuspended in sterile endotoxin-free water to a final concentration of 1.6 mg/ml. Equal volumes of DNA and lipid were incubated separately at 30°C for 5 min to equilibrate temperature. Subsequently, the lipid was gently added to the DNA. The mixture was left to complex at 30°C for 15 min.

Intranasal instillation of vector-DNA complexes. Animals were individually anesthetized with methoxyflurane (Metofane; Mallingckrodt Veterinary, Mundelein, IL) in a closed chamber and held vertically while pressure was applied to the lower mandible to immobilize the tongue and prevent swallowing. Lipid-DNA complexes (80 μg pCIhKGF complexed with 120 μg GL67 in a total volume of 100 μl) were applied dropwise onto the nostrils of the animal with a pipette, allowing the mixture to be inhaled naturally. Control animals received the same volume of lipid complexed with an irrelevant plasmid (pCF1CAT).

Systemic Gene Transfer

Preparation of lipid and DNA. Sequential injection of lipid and DNA was carried out as described by Tan et al. (60). Lipid [1,3-dioleoyl-3-trimethylammonium propane (DOTAP)/cholesterol in a 1:1 molar ratio, kindly supplied by Dr. Leaf Huang, Pittsburgh, PA] was diluted with 5% dextrose to contain 900 nmol of lipid in 100 μl. DNA (pCIhKGF or pCF1CAT) was prepared with sterile water to contain 50 μg in 100 μl.

Sequential injection of lipid and DNA. Animals were anesthetized with Avertin (2.5%, 0.1 ml/10 g), the tail was heated transiently with warm water, and 100 μl of lipid solution (900 nmol) were injected into the tail vein. Two minutes later, 100 μl of the DNA (50 μg, pCIhKGF or pCF1CAT) solution were injected in a similar manner, and the animal was left to recover from the anesthetic in a heated cage at 30°C.

TaqMan RT-PCR for Detection of Vector-Specific Expression

Whole lungs were submerged in RNAlater (Ambion, Huntingdon, Cambridgeshire, UK) and stored at 4°C until further analysis. Samples were homogenized in 4 ml of RLT (Qiagen) before extraction of total RNA using RNeasy mini protocol (Qiagen). Levels of plasmid-derived mRNA were quantified by real-time quantitative multiplex TaqMan RT-PCR using the ABI Prism 7700 Sequence Detection System and Sequence Detector version 1.6.3 software (Applied Biosystems, Warrington, Cheshire, UK). The oligonucleotide primer and fluorogenic probe sequences were designed using Primer Express Software version 1.0 (Applied Biosystems). Plasmid-specific mRNA from the pCIhKGF was quantified using forward primer (5′-GCTTCTGACACAACAGTCTCGAA-3′), reverse pCI primer (5′-GGAGTGGACACCTGCCCA-3′), and the fluorogenic pCI probe (5′-FAM-TGCCTCACGACCAACTTCTGCAGC-TAMRA-3′). 18S ribosomal RNA was quantified using Ribosomal RNA Control Reagents (Applied Biosystems).

RNA was heated to 75°C for 5 min and then reverse transcribed with TaqMan RT reagents (Applied Biosystems). The RT-reaction mix (5 μl) consisted of 1× TaqMan RT buffer, 5.5 mM $MgCl_2$, 500 μM each dNTP, 0.4 U/μl RNase inhibitor, 1.25 U/μl MultiScribe reverse transcriptase, 0.4 μM pCI reverse primer, 0.4 μM reverse rRNA primer, and ~5 ng total RNA. Reactions were incubated at 48°C for 30 min followed by 95°C for 5 min. Subsequently, triplicate 25-μl PCRs were performed for each sample. Each 25-μl reaction consisted of 1× TaqMan Universal PCR Mastermix (Applied Biosystems), 300 nM forward pCI primer, 300 nM reverse pCI primer, 100 nM pCI probe, 50 nM forward rRNA primer, 50 nM reverse rRNA primer, 50 nM rRNA probe, and 5 μl reverse-transcribed template. Reactions were incubated at 50°C for 2 min and then 95°C for 10 min followed by 40 cycles of 95°C for 15 s and 60°C for 1 min.

Controls included no template and no reverse transcriptase control in which total RNA or MultiScribe reverse transcriptase and RNase inhibitor were omitted from the reverse transcriptase reaction, respectively. Relative levels of plasmid-derived mRNA were determined using the ΔCT method (as described in Ref. 1a). In this study, the amount of pCI plasmid was normalized to 18S rRNA (endogenous reference) and expressed relative to a calibrator that was used throughout the study. The calibrator was total RNA extracted from mouse lung treated with 100 μg of pCIkLux in 150 μl via intranasal instillation (as described above) and harvested 24 h postdose.

Detection of Transgene Expression

KGF expression in lung homogenate. KGF ELISA was carried out using ELISA development reagents according to the manufacturer's recommendations (R&D Systems, Abingdon, UK). Lung homogenates (100 μl) from KGF-transfected mice or rhKGF standards were tested. Absorbance was determined in a microplate reader at 450 nm (wavelength correction 540 and 570 nm). The KGF concentration was calculated from a standard curve using known amounts of hKGF (1,000 pg/ml to 15.6 pg/ml) correlated to amount of protein detected in the lung homogenate.

Induction of Lung Injury

Male BALB/c mice (6–8 wk, 19–25 g; Harlan, Bicester, UK) were anesthetized with Avertin (2.5%, 0.1 ml/10 g). The trachea was visualized by blunt dissection, and the animal was intubated via the oral route with a 22-gauge cannula (3S Healthcare, London, UK). Mechanical ventilation (120 strokes/min, stroke volume 200 μl) was carried out using a MiniVent (type 845; Hugo Sachs Elektronik). OA (0.2 ml/kg or 0.4 ml/kg body wt; Sigma, Poole, UK) suspended in 50 μl of sterile PBS was administered through the tail vein with a 0.5-ml insulin syringe (3S Healthcare). Control animals received 50 μl of PBS. Animals were monitored for the 1-h duration of the experiment and then killed by anesthetic overdose.

Lung Wet-To-Dry Weight Ratios

Lungs were removed in toto at the end of the experiment. The trachea and esophagus were separated from the lungs by blunt dissection, and the wet weight of the latter was determined. Subsequently, the lungs were incubated at 55°C overnight to remove all moisture. The dry weight was then measured, and the ratio of wet-to-dry weight was calculated.

BAL

The animal was extubated, and a 22-gauge cannula (3S Healthcare) was inserted into the trachea. The lungs were lavaged with 500 μl of PBS three times (total volume 1.5 ml). Retrieval volume was maximized by compression of the thorax following the last lavage.

Total Cell Counts

BAL fluid (BALF) samples were centrifuged at 900 relative centrifugal force (g_{av}) for 5 min at 4°C, the supernatant was removed, and the pellet was resuspended in 100 μl of PBS. Ten microliters of the cell suspension were stained with crystal violet stain (BDH), and nucleated cells were counted in a Neubauer hemocytometer. A total of 0.5×10^6 cells in a volume of 100 μl of PBS were centrifuged (Cytospin 3; Shandon, Astmoor, UK) onto slides (700 g_{av} for 4 min)

and stained for 5 min with May and Grunwald and Giemsa stains (BDH). The slides were quantified for macrophages, neutrophils, and lymphocytes by counting a total of 200 cells/slide at ×25 magnification.

Macrophage Inflammatory Protein-2 in Lung Homogenates

Macrophage inflammatory protein-2 (MIP-2) levels were measured using a precoated murine MIP-2 colorimetric sandwich ELISA kit (R&D Systems) according to the manufacturer's recommendations. The MIP-2 concentration in the lung homogenate supernatant was calculated from a standard curve using known amounts of murine MIP-2 in a range from 7.8 pg/ml to 500 pg/ml.

BALF

Total protein and lactate dehydrogenase measurements. The total protein concentration in the BALF supernatant was measured by the Folin-Lowry method (48). Lactate dehydrogenase (LDH) levels were determined by the rate of pyruvate substrate conversion to lactate according to the manufacturer's recommendations (Sigma Diagnostics, Poole, UK).

Albumin estimation. To quantify the leak of albumin from the serum into the alveoli, the albumin concentration in the BAL supernatant was measured. This was carried out according to the manufacturer's recommendations (Sigma Diagnostics). The absorbance was measured spectrophotometrically at 628 nm (Unicam UV1; Thermo Electron Spectrometry, Cambridge, UK). The albumin concentration in the samples was calculated from a standard curve generated by using known amounts of murine albumin (Sigma) in the range of 5–100 mg/ml.

Quantification of Lung Injury

Light microscopy. All slides were coded and evaluated in a blinded fashion to prevent bias. A point scoring system was used to quantify the extent of lung injury and was defined semiquantitatively as the presence of any one of: *1*) capillary congestion; *2*) alveolar/interstitial edema; *3*) presence of fibrin; *4*) alveolar/interstitial hemorrhage; *5*) necrosis; or *6*) alveolar/interstitial neutrophils. The mean % damage score for an animal was calculated by counting a total of 24 randomly selected fields/slide (×200 magnification) for one section. For quantification, each field of view was required to contain >50% alveolar tissue.

Transmission electron microscopy. The lungs were inflated with fixative (2.5% glutaraldehyde, 50 mM sodium cacodylate buffer) in situ to a constant pressure of 25–30 cm and removed in toto into fixative and stored at 4°C for a minimum of 24 h. Samples of parenchyma of the left lobe and right upper lobe were postfixed in 1% osmium tetroxide in 50 mM sodium cacodylate buffer, dehydrated in graded alcohol and propylene oxide, and subsequently embedded in Araldite epoxy resin. Blocks were initially cut as semithin sections (1 μm) on a Reichart Ultracut E and stained with 1% toluidine blue (in 1% sodium tetraborate) for the purposes of orientation and initial morphological assessment. Ultrathin (80–100 nm) sections were cut, contrasted with uranyl acetate and lead citrate, and examined with a Hitachi 7000 transmission electron microscope.

Physiological Measurements of Lung Function: Dosing Optimization

Administration of OA for the physiological measurements of lung function was undertaken via a catheter placed in the jugular vein, as tail vein administration proved difficult and unreliable due to the experimental set up needed for lung function measurements. More efficient OA delivery is likely through the jugular compared with the tail vein. In keeping with this, administration of 0.2 ml/kg through the jugular vein resulted in 100% mortality within 1 h, equivalent to that seen with 0.4 ml/kg through the tail vein. Reduction of the jugular dose to 0.1 ml/kg prevented premature deaths over the 1-h time period, as was the case for 0.2 ml/kg administration by tail vein injection. Thus 0.1 ml/kg was used for all studies of lung mechanics and blood gas analysis.

Physiological Measurements of Lung Function

Lung physiological measurements were carried out as previously described in detail by Wilson et al. (68). In brief, male BALB/c mice (8–10 wk, 22–28 g, Harlan) were anesthetized by intraperitoneal injection of Hypnorm/Midazolam (Hypnorm:MZ:water 1:1:3, 0.1 ml/10 g) and placed in the supine position. An endotracheal cannula [0.76-mm inner diameter (ID), 1.22-mm outer diameter (OD)] was inserted via tracheotomy and secured with a suture. Animals were ventilated with a custom-made mouse jet ventilator system, as described by Ewart et al. (17). Airway pressure was monitored by a pressure transducer (MLT0380; ADInstruments, Chalgrove, UK), and airway flow was determined by a differential pressure transducer (PX137; OMEGA Engineering, Manchester, UK) connected to a miniature pneumotachogram in the ventilator circuit. A polyvinyl chloride (PVC) catheter (0.28-mm ID, 0.6-mm OD; Critchley Electrical Products, Silverwater, Australia) was introduced into the left carotid artery for monitoring arterial pressure using a pressure transducer (MLT844, ADInstruments) and measurement of blood gases. Rectal temperature was maintained between 36 and 37°C by the use of a heated pad. All data collected from the ventilator and blood pressure transducers during the experiment were recorded by PowerLab Data Recording System (ADInstruments).

After standardization of volume history of the lungs with a sustained inflation of 35 cm/H_2O for 5 s, the animals were ventilated with a tidal volume of 9–10 ml/kg, a respiratory rate of 120 breaths/min, and inspiratory:expiratory ratio of 1:2 throughout the experiment. Administration of OA was carried out via a jugular vein cutdown and cannulation. Briefly, 0.1 ml/kg of OA was loaded into 0.28-mm single-lumen PVC tubing (Critchley Electrical Products) and connected to the jugular vein line with a 30-gauge needle. OA was infused at a controlled rate using a syringe pump (0.3 ml/h, KD Scientific). Control animals received an equal volume of sterile PBS. Respiratory system compliance and resistance were measured every 15 min by the end-inflation occlusion technique. Blood gas analyses were made on serial arterial blood samples (60 μl) collected via the carotid cannula before and at 30 min and 1 h after OA administration and analyzed by a fetal scalp blood gas analyzer (Chiron Rapidlab 248; Bayer Diagnostics, Newbury, UK).

Statistical Analysis

Data are cases represented in summary plots that are based on the median, quartiles, and extreme values. The box represents the interquartile range, which contains the 50% of values. The whiskers are lines that extend from the box to the highest and lowest values, excluding outliers, which are defined separately with circles. A line across the box indicates the median. Selected data (see Figs. 3*A* and 4) are represented as dot plots or as median ± first and third data quartile (see Fig. 9). Comparison of data between groups used the Kruskal-Wallis analysis of variance for multiple unpaired, nonparametric groups, followed (where permitted) by Mann-Whitney's *U*-test, with the Bonferroni correction for multiple comparisons. The null hypothesis was rejected at $P < 0.05$.

RESULTS

rhKGF Produces A Dose- and Time-Related Increase in ATII Cells

Intratracheal instillation of rhKGF at 1–15 mg/kg body wt resulted in a significant ($P < 0.01$ for all groups) increase in SP-B-positive cells compared with animals receiving diluent

alone 2 days following administration (Fig. 1*A*). The KGF-induced increase in ATII cell numbers was dose related with a peak of proliferation following 10 mg/kg of rhKGF [23 ± 2.7 compared with 8.2 ± 1 ATII cells/field of view (×200 magnification) following administration of diluent]. Representative images of SP-B immunohistochemical staining in animals receiving the diluent alone or rhKGF at 10 mg/kg body wt are shown in Fig. 2. To ensure SP-B antibody specificity, morphological counting of ATII cells using hematoxylin and eosin-stained sections was also carried out. Significantly ($P < 0.01$) increased numbers of ATII cells were seen at all KGF doses (1 mg/kg, 15.2 ± 3.4; 5 mg/kg, 21.5 ± 5.2; 10 mg/kg, 28.4 ± 3.6; 15 mg/kg, 28.3 ± 2.2 compared with 10.1 ± 1.4 in animals receiving the diluent). In agreement with SP-B immunohistochemistry, 10 mg/kg produced the peak effect.

The time course of KGF-induced proliferation was examined using 10 mg/kg of rhKGF and resulted in significantly ($P < 0.01$) increased SP-B-stained ATII cells at *days 1*, *2*, *3*, and *7* following administration compared with control animals

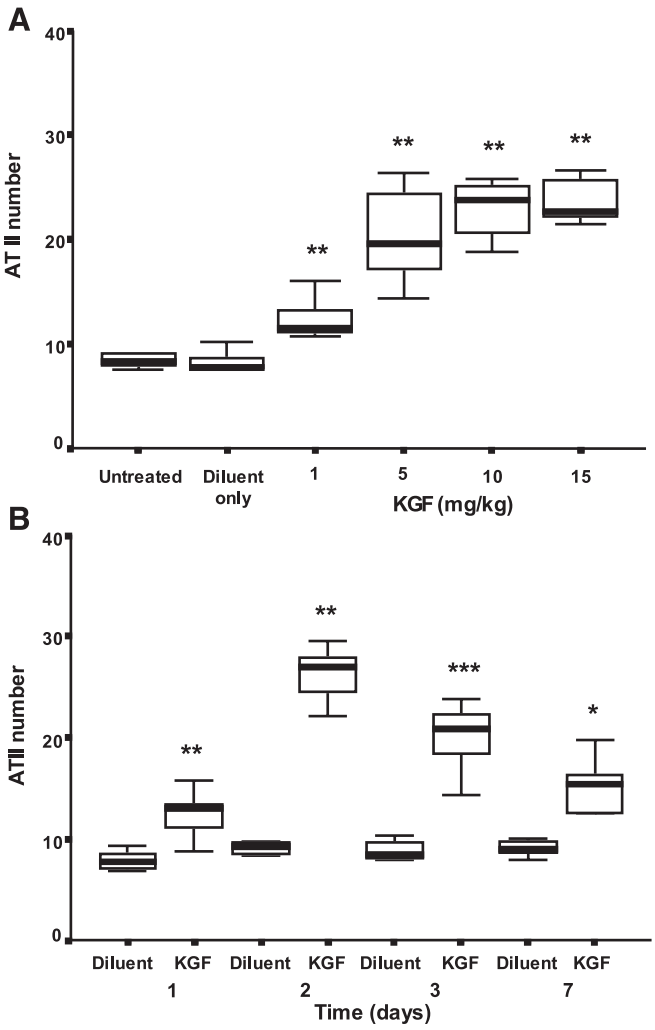

Fig. 1. Dose response (*A*) and time course (*B*) of alveolar type II (ATII) cell proliferation following intratracheal administration of recombinant human keratinocyte growth factor (rhKGF; 10 mg/kg). ATII cell numbers were determined by surfactant protein B (SP-B) immunohistochemistry ($n = 6–8$ animals for each group). *$P < 0.05$, **$P < 0.01$, and ***$P < 0.001$ compared with animals receiving the diluent only.

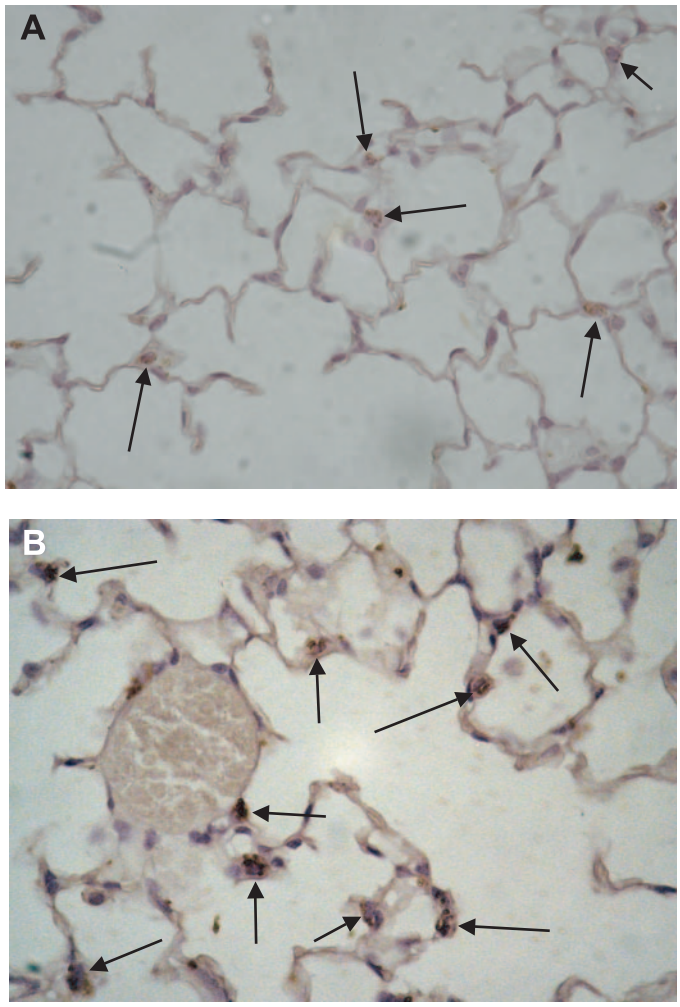

Fig. 2. Lung tissue sections (×400) stained with SP-B immunohistochemistry from control mice receiving diluent only (*A*) or 10 mg/kg of rhKGF (*B*). Arrows indicate ATII cells.

receiving diluent alone (Fig. 1*B*). The number of SP-B-positive cells peaked at *day 2* following rhKGF administration [26.0 ± 2.7 compared with 9.0 ± 0.6 ATII cells/field of view (×200 magnification) in animals receiving diluent alone]. By *day 7*, ATII cells counts were significantly ($P < 0.01$) decreased compared with *day 2* (15.4 ± 2.3 ATII cells/field of view) but were still significantly ($P < 0.05$) increased compared with control animals at the same time point.

To exclude rhKGF-induced toxicity, hematoxylin and eosin-stained tissue sections from animals receiving 1, 5, 10, and 15 mg/kg of rhKGF obtained at *day 2* were examined for the presence of edema, hemorrhage, and neutrophils. Approximately 10% of the total area from each lung section was found to include one or more of the above-mentioned parameters. However, no increase in lung damage compared with control animals was demonstrable in lung tissue following rhKGF administration (data not shown).

Topical Administration of Liposome-KGF DNA Complexes Produces KGF mRNA, Protein, and ATII Cell Proliferation

mRNA. To circumvent the problem of detection of contaminating plasmid DNA, pCI-specific mRNA was amplified by

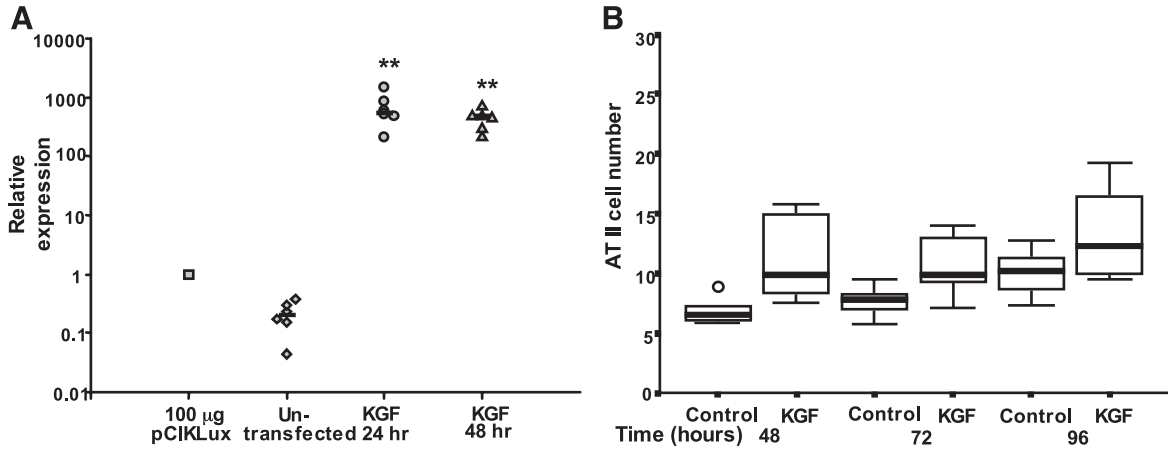

Fig. 3. Shown is pCI-specific *Taq*Man PCR amplification following intranasal instillation of pCIhKGF/GL67 (*A*, 80 μg). Relative expression is compared with intranasal instillation of a known standard, 100 μg of pCIKLux ($n = 6$ animals for each group). $^{**}P < 0.01$ compared with untransfected animals. Note log scale of *y*-axis. ATII cell quantification is shown using SP-B immunohistochemistry following intranasal liposome-mediated (GL67) gene transfer of pCIhKGF (*B*, 80 μg; $n = 6$ animals for each group).

*Taq*Man PCR, and relative expression was calculated by comparison to expression levels following intranasal instillation of a known standard (100 μg pCIKLux). Significant ($P < 0.01$) relative expression of pCIhKGF-specific mRNA was demonstrated 24 and 48 h following intranasal administration of 80 μg of pCIhKGF complexed with GL67 compared with untransfected animals (Fig. 3*A*).

Protein. In lung homogenate, low levels of KGF were detected in pCIhKGF/GL67-transfected animals by ELISA (21.5 ± 5.7 pg/mg protein at 48 h and 21.5 ± 13.8 pg/mg protein at 72 h), with a threshold sensitivity level of the ELISA of 5 pg/ml.

ATII cell quantification. Intranasal instillation of pCIhKGF/GL67 (80 μg) did not result in significantly increased ATII cell numbers as quantified by SP-B immunohistochemistry (Fig. 3*B*). However, morphological ATII cell counts revealed a significant ($P < 0.05$) increase in ATII cell numbers 72 and 96 h following intranasal transfection [15.2 ± 4.4 and 15.3 ± 3.9 ATII cells/field of view (×200 magnification) compared with 8.1 ± 1.9 in animals receiving an irrelevant plasmid].

Systemic Administration of Liposome-KGF DNA Is Toxic But Able To Produce KGF mRNA and ATII Cell Proliferation

Lipid-mediated gene transfer resulted in high mortality (15–40%) after intravenous injection in both pCIhKGF- and pCF1CAT-transfected animals. Thus group sizes were not consistently large enough to allow for statistical analysis.

mRNA. pCI-specific mRNA was amplified by *Taq*Man PCR, and relative expression was calculated by comparison to expression levels following intranasal instillation of a known standard (100 μg of pCIKLux). Significant ($P < 0.01$) relative expression of pCIhKGF-specific mRNA was demonstrated 8 and 24 h following intravenous administration of pCIhKGF (50 μg) and 2 min after injection of 900 nmol of DOTAP/cholesterol compared with untransfected animals (Fig. 4*A*).

Protein. KGF could not be detected in homogenate following intravenous transfection with pCIhKGF/DOTAP/cholesterol.

ATII cell quantification. Sequential intravenous gene transfer of pCIhKGF/lipid was associated with an increase in ATII cell numbers 48, 72, and 96 h after transfection as demon-

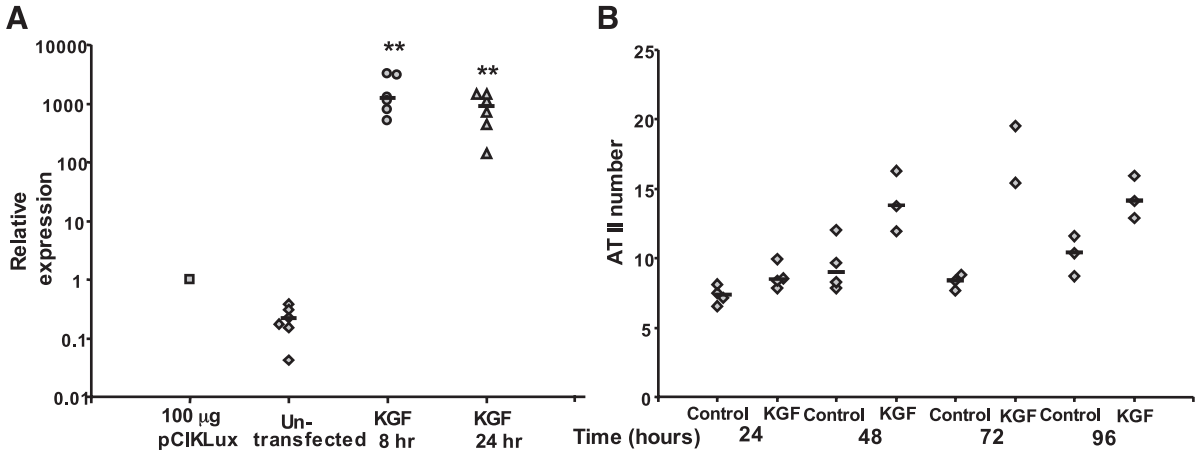

Fig. 4. Shown is pCI-specific *Taq*Man PCR amplification following sequential intravenous injection of 1,3-dioleoyl-3-trimethylammonium propane (DOTAP)/cholesterol and pCIhKGF (*A*, 50 μg). Relative expression is compared with intranasal instillation of a known standard, 100 μg of pCIKLux ($n = 6$ animals for each group). $^{**}P < 0.01$ compared with untransfected animals. Note log scale of *y*-axis. ATII cell quantification is shown using SP-B immunohistochemistry following intravenous delivery of DOTAP/cholesterol and pCIhKGF (*B*, 50 μg; $n = 2$–4 for each group).

strated by SP-B immunohistochemistry (Fig. 4*B*). However, due to the high mortality following intravenous gene transfer, the number of animals in each group was low, and statistical testing was not appropriate. A similar trend was observed following morphological counts [12.4 ± 1.4 at 24 h, 14.4 ± 2.7 at 48 h, 14.3 ± 1.9 at 72 h, 17 ± 0.3 at 96 h compared with 8.7 ± 1 ATII cells/field of view (×200 magnification) in animals receiving an irrelevant plasmid]. Pooling of data obtained from all time points (24, 48, 72, and 96 h) showed a significant ($P < 0.01$) increase in ATII cell numbers by SP-B immunohistochemistry (12.9 ± 3.7 ATII cells/field of view compared with 8.7 ± 1.6 in controls animals), which was supported by morphological assessment (14.3 ± 2.3 ATII cells/field of view compared with 8.6 ± 2.2 in control animals).

OA Produces A Dose-Related Increase in ALI

Macroscopic changes following OA administration. A dose-related difference in mortality was observed in animals treated with 0.2 and 0.4 ml/kg of OA, respectively. The higher dose was associated with 100% mortality, with death usually occurring 30–40 min following OA administration. The animals appeared cyanotic, and bloody fluid spilled out of the trachea upon extubation. At postmortem, the lungs were grossly enlarged, and severe hemorrhage affected nearly all of the lung surface. In contrast, no deaths occurred within 1 h following administration of 0.2 ml/kg of OA. At this dose, the injury appeared patchy and less severe and was commonly found at the periphery of the lung lobes. The lungs were enlarged, and bloody fluid was often found in the trachea.

Wet-to-dry weight ratios. Intravenous administration of OA (0.2 and 0.4 ml/kg body wt) was associated with a significant ($P < 0.01$) increase in the lung wet-to-dry weight ratios (Fig. 5*A*) compared with ventilated control animals receiving only PBS. This effect was not dose related. Furthermore, compared with untreated nonventilated animals, control animals that were ventilated and received intravenous PBS also had significantly ($P < 0.01$) increased wet-to-dry weight ratios.

BALF cell counts. BALF total cell counts were significantly increased in animals treated with 0.2 ($P < 0.001$) and 0.4 ml/kg ($P < 0.01$) of OA compared with control animals receiving intravenous PBS alone (Fig. 5*B*). Again, ventilated PBS-treated animals also had significantly ($P < 0.05$) increased cell counts compared with nonventilated animals. Differential cell counts showed a small increase in % neutrophils (0.2 ml/kg, 3.3 ± 0.4% compared with 1.3 ± 0.4%, $P < 0.05$; 0.4 ml/kg, 1.25 ± 0.31%) compared with PBS controls. MIP-2, a proinflammatory cytokine that is chemotactic for neutrophils, was detected by ELISA in lung homogenates from animals treated with 0.2 ml/kg of OA and was significantly ($P < 0.01$) increased compared with untreated baseline animals (135.3 ± 21.4 pg/mg of protein compared with 32.2 ± 8.8 pg/mg of protein) but was not increased following 0.4 ml/kg of OA (60 ± 15.4 pg/mg of protein).

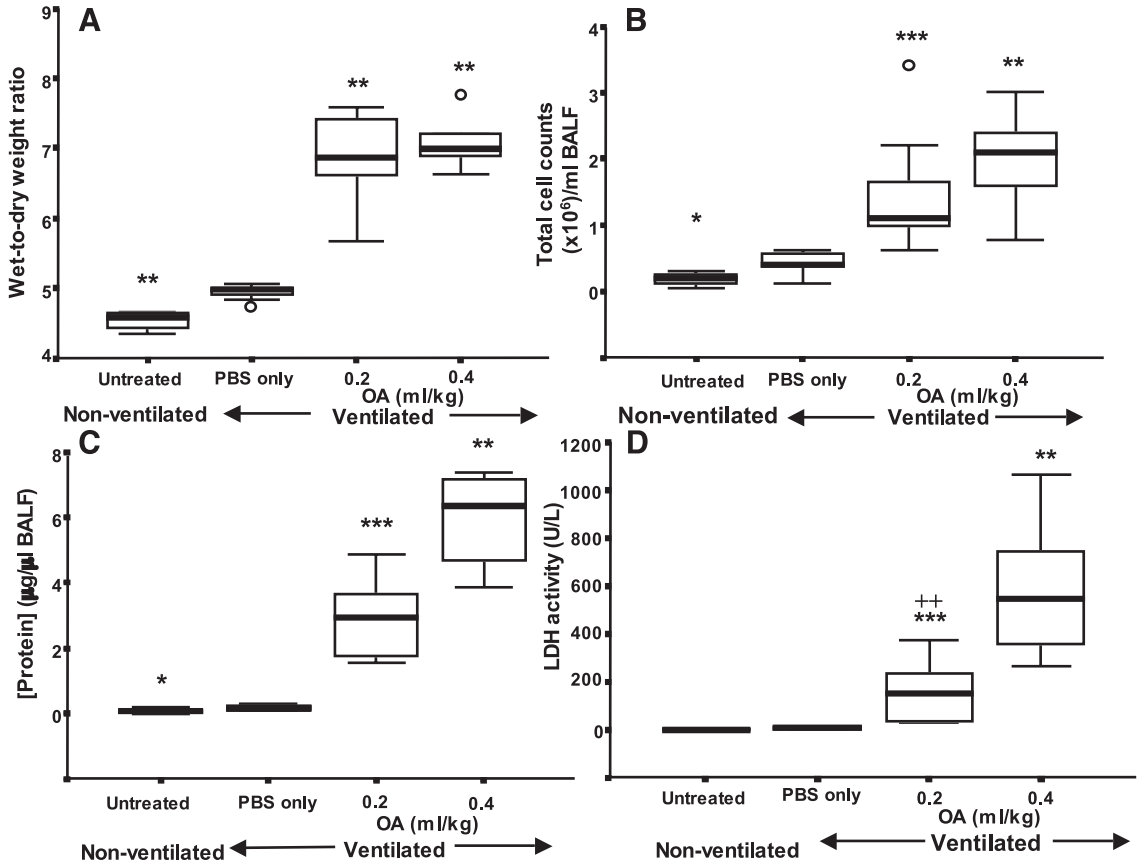

Fig. 5. Lung wet-to-dry weight ratio (*A*), total cell counts (*B*), protein (*C*), and lactate dehydrogenase (LDH) activity (*D*) in bronchoalveolar lavage fluid (BALF) following intravenous oleic acid (OA); $n = 6$–9 each group. *$P < 0.05$, **$P < 0.01$, and ***$P < 0.001$ compared with ventilated, PBS-injected controls; $^{++}P <$ 0.01 compared with 0.4 ml/kg of OA.

BALF protein and LDH. Administration of OA was associated with a dose-related increase in total protein concentration measured in BALF supernatants (Fig. 5*C*). Thus compared with control animals receiving PBS alone, BALF total protein was significantly ($P < 0.001$ and 0.01, respectively) higher in animals receiving the 0.2 and 0.4 ml/kg of OA. Again, compared with baseline untreated animals, a small but significant ($P < 0.01$) increase in total BALF protein was detected in ventilated animals that received PBS alone. This was associated with an increase in BALF supernatant albumin (0.2 ml/kg OA, 0.25 ± 0.00 μg/μl; 0.4 ml/kg OA, 0.25 ± 0.00 μg/μl compared with undetectable levels in control animals). BALF supernatant LDH activity, a marker of local cell damage, was significantly ($P < 0.01$) increased in a dose-related manner in animals injected with OA (Fig. 5*D*) compared with ventilated control animals given PBS alone.

Lung histology. Compared with untreated animals and ventilated PBS controls, OA (0.4 ml/kg) induced a significant ($P < 0.01$) increase in histological lung damage (Fig. 6). The principal histological changes seen included the presence of fibrin in the alveolar spaces, hemorrhage, and necrosis of alveolar tissues (Fig. 6*B*). Whereas alveolar fibrin, hemorrhage, and necrosis were barely detectable in sections examined from the lungs of untreated or PBS control animals (Fig. 6A), all three features were significantly ($P < 0.05$) increased in lung sections from the OA-treated animals (Fig. 6*C*).

To allow for a more detailed analysis of the lung injury induced by intravenous OA (0.2 ml/kg), lungs were assessed by transmission electron microscopy (TEM). In addition to the fibrin formation within the alveolar spaces (Fig. 7*A*), also seen by light microscopy, areas in which the entire alveolar architecture had been damaged were evident by TEM (Fig. 7, *B* and *C*). These were characterized by congested and grossly swollen capillaries, and sloughing of necrotic ATI cells, leaving a denuded basement membrane. Additionally, some endothelial damage and necrosis was evident (Fig. 7*C*). The alveolar structure was severely altered, and the destroyed epithelium had apparently undergone sloughing in large fragments.

Blood gases and lung compliance. Animals undergoing lung physiological measurements demonstrated a marked decrease in arterial P_{O_2} (Pa_{O_2}, Fig. 8*A*) within 30 min of OA administration, which further declined by 1 h. This was associated with marked increases in arterial P_{CO_2} (Pa_{CO_2}) during the 1-h period (Fig. 8*B*). No changes in arterial blood gases were evident in ventilated PBS control animals observed under similar conditions for 1 h. In addition, OA administration was associated with a progressive decrease in compliance (Fig. 8*C*) over 1 h.

Effect of rhKGF Pretreatment on OA-Induced Lung Injury

BALF cell counts. Pretreatment with rhKGF (10 mg/kg) did not significantly affect the total cell numbers found in the BALF (KGF, $2 \times 10^6 \pm 2.4$/ml of BALF, diluent, $2.6 \times 10^6 \pm 1.8$/ml of BALF) or MIP-2 levels (KGF, 15.1 ± 5.5 pg/mg of protein, diluent, 15.4 ± 3.5 pg/mg of protein).

BALF protein and LDH. No significant differences were observed in the BALF protein concentration (KGF, 11.5 ± 4.3 μg/μl; diluent, 11.6 ± 5.3 μg/μl), albumin (KGF, 9.3 ± 3.1 μg/μl; diluent, 7.1 ± 4.2 μg/μl), and LDH activity (KGF, 790 ± 522 U/l; diluent, 1,138 ± 581 U/l) in animals pretreated with rhKGF 48 h before OA.

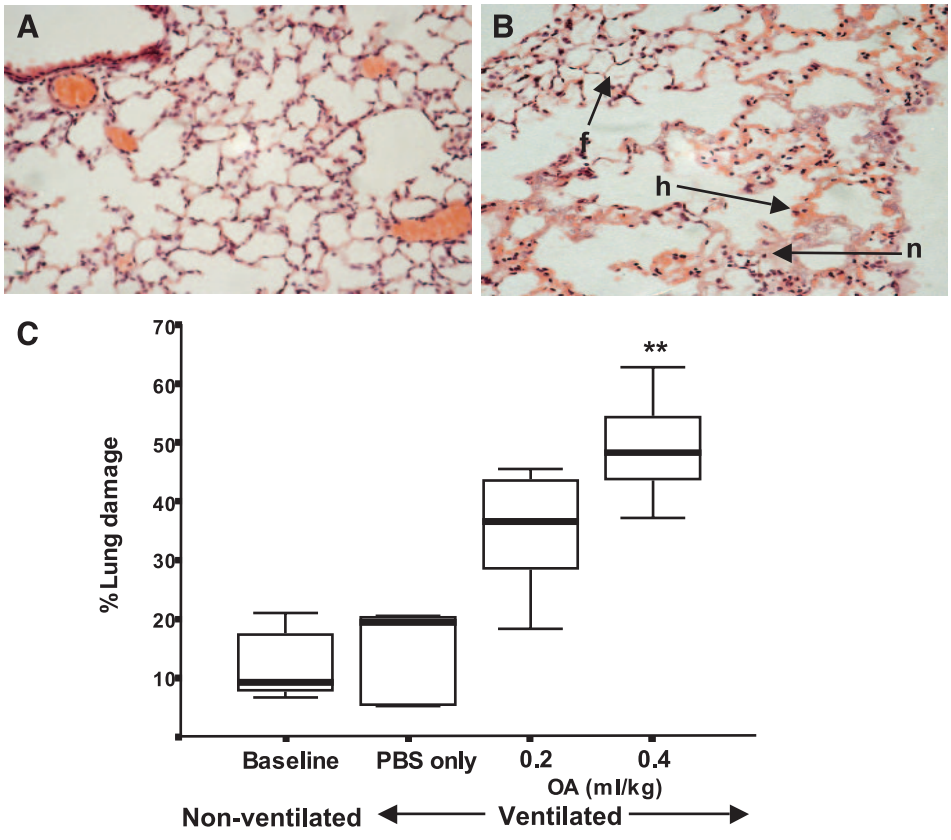

Fig. 6. Histological quantification of lung injury following intravenous OA ($n = 6$ animals for each group). Sections of hematoxylin and eosin-stained lung tissue were examined under light microscopy, and damage was recorded using the parameters described in MATERIALS AND METHODS. *A*: section from control animals receiving intravenous PBS (×200) showing alveolar spaces free of cell debris and fibrin, with no evidence of hemorrhage or necrosis. *B*: OA administration (0.2 ml/kg) results in the appearance of hemorrhagic (h) and necrotic (n) areas (×200). These areas also contain high levels of fibrin (f). Sections are representative of 6 animals examined per group. *C*: overall % damage per animal was calculated as a mean of 24 fields/slide (1 slide/animal). $^{**}P < 0.01$ compared with PBS-injected control animals.

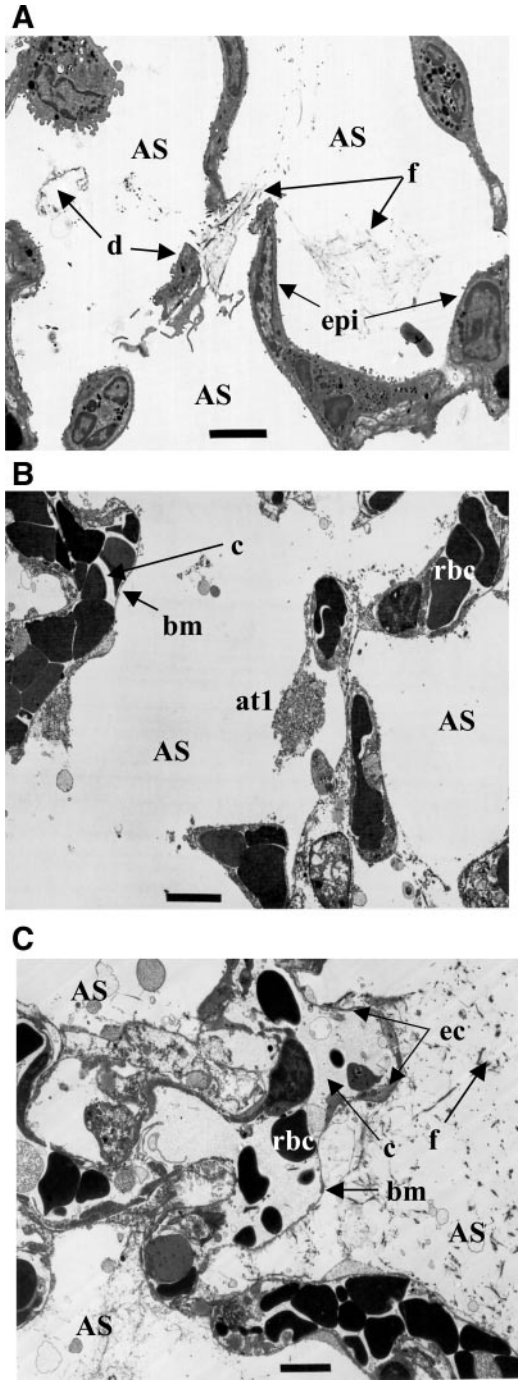

Fig. 7. Transmission electron micrographs of alveolar tissues following intravenous OA (0.2 ml/kg) are shown. *A*: alveolar epithelium (epi) and endothelium appear intact, but the alveolar space (AS) contains fibrin (f) and cellular debris (d). *B*: area showing more severe injury. Capillaries (c) appear swollen with abnormally shaped red blood cells (rbc). The epithelial basement membrane (bm) is denuded in large areas caused by loss of ATI (at1) cells. A necrotic AT1 can be seen detaching from the bm. *C*: extensive loss of alveolar architecture. Large fragments of AT1 cells have detached from the basement membrane, and capillaries are grossly enlarged and show some necrotic endothelial cells (ec) and denudation of both the epithelial and endothelial basement membrane. All sections, ×1,500; bar = 5 μm. Micrographs are representative of 3 animals.

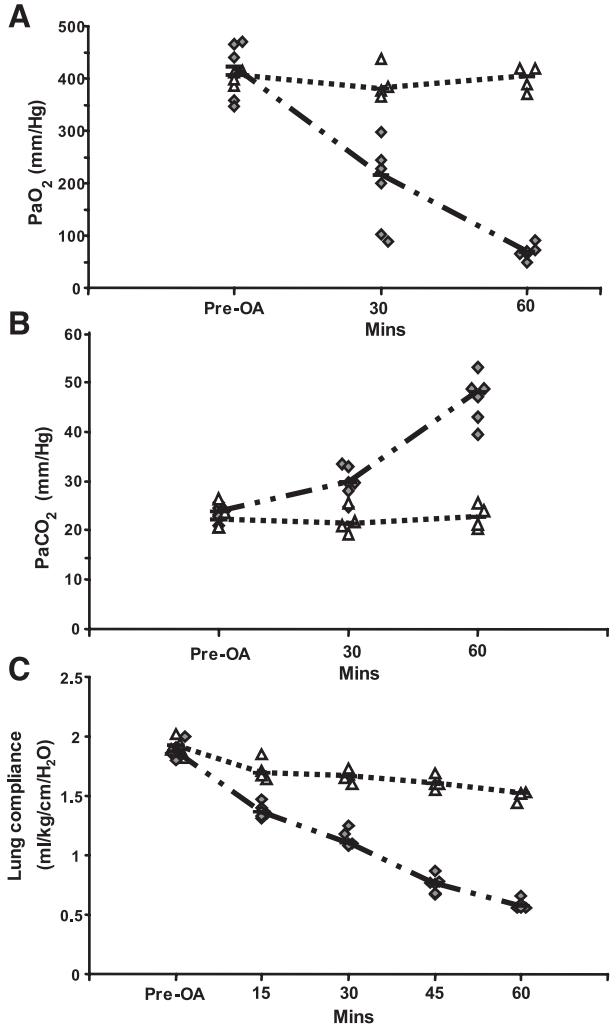

Fig. 8. Effect of intrajugular OA on blood gases and lung compliance. ◆, OA (0.1 ml/kg, $n = 6$); △, PBS-injected control animals ($n = 4$). *A*: arterial P_{O_2} (Pa_{O_2}, mmHg). *B*: arterial P_{CO_2} (Pa_{CO_2}, mmHg). *C*: lung compliance ($ml \cdot kg^{-1} \cdot cmH_2O^{-1}$). Solid black line indicates median. Each symbol represents 1 animal.

Lung histology. No improvements were observed in histological damage in KGF-pretreated OA-injured animals (KGF, 60 ± 12% lung damage; diluent, 43 ± 14% lung damage).

Blood gases and lung compliance. Pretreatment of mice with rhKGF (10 mg/kg) 48 h before intra-jugular OA (0.1 ml/kg) challenge resulted in a significant ($P < 0.001$ and $P < 0.05$, respectively) improvement in arterial P_{O_2} 30 and 60 min after OA administration compared with control mice receiving the diluent only (Fig. 9*A*). Additionally, rhKGF pretreatment was associated with significantly ($P < 0.01$) decreased arterial P_{CO_2} 30 and 60 min after OA administration (Fig. 9*B*) compared with diluent only. Lung compliance was significantly ($P < 0.01$) improved in animals pretreated with rhKGF (Fig. 9*C*).

DISCUSSION

We have shown that intratracheal rhKGF administration in mice resulted in a marked dose-related proliferation of ATII cells. However, whereas topically administered lipid-mediated gene transfer resulted in KGF mRNA production, KGF could

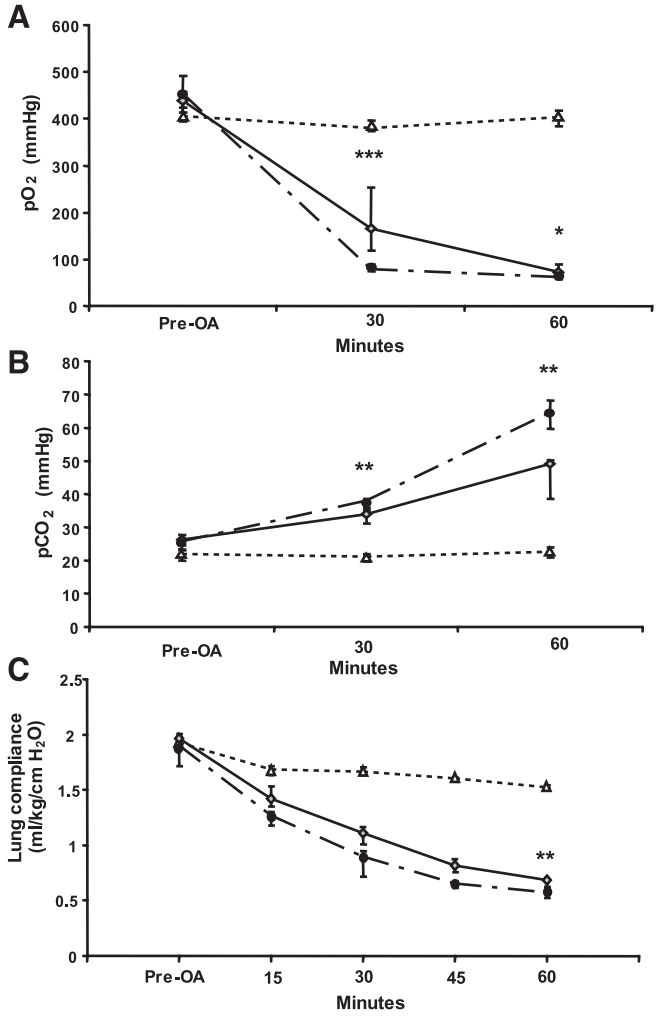

Fig. 9. Effect of rhKGF (10 mg/kg, 48-h pretreatment) on arterial blood gases (*A* and *B*) and lung compliance following intrajugular OA (*C*). rhKGF pretreatment (10 mg/kg, 48 h) + OA (0.1 ml/kg, $n = 12$); diluent-only pretreatment [48 h + OA (0.1 ml/kg, $n = 12$)]; PBS control (no OA, $n = 4$). *A*: arterial P_{O_2} (Pa_{O_2}, mmHg). *B*: arterial P_{CO_2} (Pa_{CO_2}, mmHg). *C*: lung compliance. Data are expressed as median ± first and third data quartile. $^*P < 0.05$, $^{**}P < 0.01$, and $^{***}P < 0.001$ compared with animals receiving the diluent only at the same time point.

not be detected in lung tissue, and only a modest effect was seen on ATII cell proliferation. To assess the potential for KGF therapy, we subsequently characterized a mouse model of ALI, showing features characteristic of the disease in humans. Finally, we assessed whether rhKGF could ameliorate the pathophysiology. Significant improvements were observed in arterial blood gases and lung compliance. These data demonstrate, for the first time, that rhKGF pretreatment can improve the clinical surrogates of ALI.

The mouse remains an important model system with transgenic technology making it possible to study effects of a single gene on the whole organism. Additionally, gene delivery methods and gene transfer efficiency have been well characterized in the mouse. This study has for the first time characterized the KGF response in this species in detail. Intratracheal instillation of 5 mg/kg body wt has been used most frequently in experimental ALI studies in both mice and rats (55, 65, 71, 73, 74). We confirmed that this dose is associated with significant ATII cell proliferation 2 days after administration. However, administration of 10 mg/kg appeared to result in higher and less variable ATII cell numbers. Studies in the rat have demonstrated ATII proliferation to be focal and thus resulting in piles of ATII cells within the alveoli (63). However, significant evidence of focal proliferation was not observed in this study, and cell proliferation in the lung sections from KGF-treated animals appeared to be diffuse. Furthermore, we demonstrated that ATII cell numbers were still increased at *day 7* after administration, in contrast to Ulich et al. (63), who showed resolution of proliferation in rats. The administered dose was 5 mg/kg of rhKGF, and thus it is possible that the higher KGF dose used in this study extends the ATII cell proliferative response.

Novel interventions for ALI are needed as mortality remains high, even in well-equipped intensive care units. A number of studies have recently demonstrated the possibility of gene therapy as a potential intervention, particularly addressing the inflammatory aspects of ALI, using IL-10 (38, 41), elafin (54), neutrophil inhibitory factor (77), and heme oxygenase-1 (25, 45). However, no studies to date have used gene transfer to address alveolar repair following ALI.

Nonviral KGF Gene Delivery Results in Modest ATII Cell Proliferation

GL67 was first described in 1996 by Lee et al. (31), who demonstrated a 100-fold increase in reporter gene expression following intranasal transfection in mice compared with other first-generation cationic liposomes. Expression was found to peak 48 h following intranasal delivery of 80 μg of DNA. Although high levels of CAT reporter gene activity were demonstrated in lung homogenate 24–72 h following intranasal administration of pCF1CAT/GL67 complexes, significant KGF levels could not be detected in parallel studies using pCIKGF/GL67 despite evidence for gene transfer. In keeping with this, no increase in SP-B-positive cells was seen, with only a small increase in the numbers of ATII cells assessed by routine histology. Systemic lipid-mediated gene transfer has been demonstrated to transfect primarily pulmonary endothelial cells (32). However, KGF produced by capillary endothelial cells as a result of systemic gene transfer may reach across the alveolar endothelial-epithelial barrier, thus stimulating ATII cell proliferation. Lipid (DOTAP/cholesterol)-protamine sulfate-DNA (LPD) has previously been shown to be effective for intravenous lung delivery (32) but also has toxic effects. The toxicity is caused by a strong inflammatory response to the unmethylated CpG motifs in the DNA following uptake of LPD by circulating immune cells, primarily resulting in high levels of TNF-α and IFN-γ (34). Recently, reduced toxicity and increased gene transfer efficiency have been demonstrated by sequential delivery into the tail vein of cationic liposomes followed by DNA (60). Administration of the lipid before the DNA is believed to increase the retention time of plasmid DNA within the lung capillaries (33). However, the toxicity caused by systemic gene transfer was confirmed in this study, as mortality was high. In surviving animals, quantitative RT-PCR confirmed the expression of pCI-specific mRNA 8 and 24 h following systemic transfection. However, KGF could not be detected in lung homogenate or serum following intravenous pCIhKGF/DOTAP/cholesterol gene transfer at any time points.

Although a clear trend toward an increase in ATII cell numbers was observed following sequential intravenous gene transfer, significance was not tested due to the low numbers in each group. However, by grouping the data from the different time points, a highly significant increase in ATII cell numbers could be demonstrated. As mentioned above regarding topical gene delivery, the resulting ATII cell numbers achieved by systemic gene transfer were lower than those resulting from delivery of KGF protein. Additionally, in the light of the high mortality observed in these experiments, systemic KGF gene transfer is currently not an appropriate strategy for evaluating the protective effect in of KGF gene transfer in the OA model of ALI. We conclude that at present, nonviral lung gene transfer by topical and systemic administration cannot match the efficacy of recombinant protein. Virus-mediated gene transfer, using vectors such as adenovirus, would likely have resulted in more efficient gene transfer. However, the significant inflammatory response associated with viral delivery would be detrimental in the ALI setting.

Intravenous OA in Mouse Results in Severe Alveolar Injury

The oleic acid model is regarded as relevant for ARDS and has been extensively characterized in many larger animal species, including sheep, pigs, dogs, rats, and rabbits. Intravenous OA infusion causes severe pulmonary edema in a number of species due to an increase in the pulmonary alveolar barrier permeability. The arrest of small OA microemboli in the pulmonary capillaries results in severe congestion and hemorrhage (10). This microinfarction results in extensive necrosis of the alveolar epithelial type I cells (39) and also affects the permeability of endothelial cells (26). Neutrophil infiltration, fibrin deposition, and hyaline membrane formation are also common features (15, 40). These pathological events lead to hypoxemia and severely compromised lung compliance (9).

There is only one previously reported study of OA administration in mice (56). Although poorly characterized, the pathophysiology described was similar to that seen in other animal species. In our study, intravenous OA administration in mice resulted in severe pulmonary edema and a dose-related increase in BALF total protein concentration, likely representative of a combination of serum protein leakage (24), inflammatory cells, and necrotic alveolar epithelial cells (10). Further measurement of BALF supernatant albumin levels, however, suggested that leaked serum protein contributed only ~10% of the total BALF protein levels with the majority likely to originate from protein debris released from necrotic alveolar cells. This is supported by the significant increases in BALF total cell counts and by LDH levels in BALF supernatant as well as the finding of marked alveolar epithelial cell necrosis on TEM analysis. TEM analysis also demonstrated the presence of some endothelial injury and necrosis, which would further contribute to the overwhelming pulmonary edema and the albumin found in the BALF supernatant.

Acute OA Does Not Result in Inflammatory Cell Infiltration

Surprisingly, differential cell counts demonstrated only a small (albeit significant) increase in neutrophil numbers at 1 h following 0.2 ml/kg of OA. This finding contrasted with other studies in which OA was shown to cause a marked influx of neutrophils into the alveoli 4 h after OA administration (53). It is possible that transepithelial neutrophil migration does not occur within the initial hour after OA administration, and had we measured later time points, increased BAL neutrophils may have been detected (15). This possibility was supported by a significant increase in MIP-2 following OA (0.2 ml/kg) compared with untreated baselines in which no MIP-2 was detected. MIP-2 has potent neutrophil chemotactic activity and is secreted by epithelial cells as a key mediator of neutrophil recruitment in response to tissue injury (14). Thus the significant increase demonstrated in total BAL cell counts is likely to be a result of the presence of sloughed necrotic epithelial cells.

Mechanism of OA Injury Differs from ARDS

The OA mouse model has a number of dissimilating features to human ARDS. First, the initiating events leading to OA-induced lung injury do not resemble the clinical situation. ARDS generally results from sepsis or multiple injuries and evolves secondary to an overwhelming inflammatory cascade. OA-induced lung damage is likely to be caused by OA microemboli being trapped in the capillary bed, causing subsequent local necrosis followed by inflammation. Second, the time course of OA-induced injury development and progression is much shorter than that of human ARDS. The acute phase of human ARDS develops over 1–7 days and is also characterized by extensive damage to the alveolar epithelium, hemorrhage, and pulmonary edema, leading to severely decreased lung compliance and hypoxemia (3, 61). However, with a view to evaluating KGF as a potential therapy for alveolar epithelial repair, this model consistently reproduces the histopathological features of ARDS.

Mechanical Ventilation Causes Some Degree of Lung Injury

Compared with untreated baseline animals, a significant increase in wet-to-dry weight ratios was also observed in ventilated control animals given intravenous PBS. This suggests that mechanical ventilation is associated with the development of at least some degree of the pulmonary edema observed following OA administration and confirms previous observations that mechanical ventilation causes lung injury (42, 64), including increased microvascular permeability and leakage of fluid into alveolar spaces (23). Ventilator-induced lung injury may be partly attributed to the effects of excessive airway pressure and overdistension of the alveoli during ventilation (13). It is, however, important to distinguish the above studies of lung injury caused by deliberate hyperventilation from this study, where the injury is most likely caused by dry gas ventilation and atelectasis due to low positive end-expiratory pressure (PEEP) and inadequate alveolar recruitment procedures. In these experiments, no PEEP was applied, which may affect lung expansion and exacerbate edema formation during mechanical ventilation (12). The addition of PEEP in the ventilatory strategy prevents complete alveolar collapse and reopening repeatedly during the breathing cycle and thereby reduces the shear stress forces generated.

rhKGF Improves Gas Exchange and Lung Compliance in OA-Injured Mice Without Evidence of Increased Epithelial Repair

Pretreatment of mice with intratracheal rhKGF (10 mg/kg) 48 h before intrajugular administration of OA (0.1 ml/kg)

resulted in a significant improvement in Pa_{O_2} 30 and 60 min after OA administration. The improvement in Pa_{CO_2} was significant 30 and 60 min after OA administration. Lung compliance was also significantly improved in animals pretreated with rhKGF and was observed as early as 15 min after OA administration. However, by comparison of the lung physiological results from rhKGF-pretreated animals to ventilated animals not receiving OA, it becomes clear that the KGF-induced improvements are relatively small. It is possible that the existing pool of ATII cells generated by the rhKGF pretreatment reduces the extent of epithelial damage caused by OA, thereby increasing gas exchange and improving the mechanics of the lung. Additionally, intratracheal rhKGF pretreatment may increase cell migration rate, cell spreading, and adherence, as described by Waters and Savla (66) and Atabai et al. (2), to repair areas of denuded basement membrane. However, whether this is likely to occur within the short time course of OA injury in this model is not known. Some evidence exists demonstrating that tracheal epithelial cells can migrate minutes after wound induction in vivo (16), but whether this occurs in alveolar epithelial cells is not known.

Pretreatment of the animals with rhKGF did not appear to ameliorate the extent of protein exudation (BALF protein and albumin), epithelial cell damage (LDH activity), or cellular infiltrate (BALF cell counts) induced by OA. Additionally, KGF pretreatment did not protect against the histological damage induced by OA, and no differences in fibrin, hemorrhage, or necrosis were detected. These findings were surprising in light of the physiological improvements demonstrated. Intrajugular administration of 0.1 ml/kg of OA in mice produces very acute and severe lung injury, resulting in damage to >40% of the lung tissue. The injury may have been too severe to detect any changes in the pathological end points, and further titration of the OA dose to result in a less acute and overwhelming lung injury may reveal an effect of rhKGF pretreatment on the less sensitive pathological end points. Furthermore, there may have been alternative mechanisms underlying the physiological improvements seen. Some studies have demonstrated increased surfactant protein production following KGF administration (72), most likely due to the hyperplasia of ATII cells. This increase in surfactant production may have helped to improve gas exchange and lung compliance by preventing alveolar collapse in the early stages of OA-induced lung injury development but would not alter the pathological and histological features of OA-induced lung injury. Additionally, KGF may have increased the number of Na^+K^+-ATPase pumps, as has previously been demonstrated (6), thus reducing fluid accumulation within the alveoli. Nevertheless, the results raise questions regarding the relevance of the improvements seen in the mice to the clinical picture of ALI and ARDS. It may be possible that a small, but significant, improvement in gas exchange may not be accompanied by a measurable reduction in damage to the alveolar epithelial membrane but may be sufficient to prevent morbidity/mortality by reducing the amount of time spent on mechanical ventilation. Additionally, prolonging the time KGF is present in the lung tissue may enhance the protective effect observed. Whereas we have established that a single dose of intratracheal administration of 10 mg/kg of rhKGF appears to produce the maximum ATII proliferative effect, multiple rhKGF administrations may further improve the protective effect. Finally, it is possible that prolonged expression achieved by gene transfer with a vector expressing high levels of KGF may result in enhanced protective effects.

The potential of ameliorating ALI by KGF pretreatment has been confirmed in this study using a murine model of very severe ALI. Whereas KGF did not appear to directly affect alveolar epithelial repair and integrity, measurements of blood gases and lung compliance demonstrated significant improvements in gas exchange, possibly linked to increased presence of surfactant proteins secreted from proliferating ATII cells. Further optimization of the OA model with respect to time course and dosing may reveal histological and pathological improvements.

ACKNOWLEDGMENTS

We gratefully acknowledge Amgen (Thousand Oaks, CA) for supplying recombinant human KGF, Stuart Aaronson (Derald H. Ruttenberg Cancer Center, Mount Sinai School of Medicine, New York, NY) for providing human *KGF* DNA, and Dr. Michael Wilson (Dept. of Anaesthetics and Intensive Care, Chelsea and Westminster Hospital, Faculty of Medicine, Imperial College London) for assistance in murine pulmonary function testing.

GRANTS

This study was partly supported by Medical Research Council Grant G0000101 and Wellcome Trust Grant 057459.

REFERENCES

1. **Adamson IYR and Bowden DH.** The type II cell as progenitor of alveolar epithelial regeneration. *Lab Invest* 30: 35–42, 1974.
1a. **Applied Biosystems.** In: *User Bulletin no 2: ABI PRISM 7700 Sequence Detection System*, 1997, p. 11–13, 22–23.
2. **Atabai K, Ishigaki M, Geiser T, Ueki I, Matthay MA, and Ware LB.** Keratinocyte growth factor can enhance alveolar epithelial repair by nonmitogenic mechanisms. *Am J Physiol Lung Cell Mol Physiol* 283: L163–L169, 2002.
3. **Bachofen M and Weibel ER.** Alterations of gas exchange apparatus in adult respiratory insufficiency associated with septicemia. *Am Rev Respir Dis* 116: 589–615, 1977.
4. **Bachofen M and Weibel ER.** Structural alterations of the lung parenchyma in the adult respiratory distress syndrome. *Clin Chest Med* 3: 35–56, 1982.
5. **Barazzone C, Donati YR, Rochat AF, Vesin C, Kan CD, Pache JC, and Piguet PF.** Keratinocyte growth factor protects alveolar epithelium and endothelium from oxygen-induced injury in mice. *Am J Pathol* 154: 1479–1487, 1999.
6. **Borok Z, Danto SI, Dimen LL, Zhang XL, and Lubman RL.** Na^+-K^+-ATPase expression in alveolar epithelial cells: upregulation of active ion transport by KGF. *Am J Physiol Lung Cell Mol Physiol* 274: L149–L158, 1998.
7. **Chelly N, Mouhieddine-Gueddiche OB, Barlier-Mur AM, Chailley-Heu B, and Bourbon JR.** Keratinocyte growth factor enhances maturation of fetal rat lung type II cells. *Am J Respir Cell Mol Biol* 20: 423–432, 1999.
8. **Danilenko DM, Ring BD, Yanagihara D, Benson W, Wiemann B, Starnes CO, and Pierce GF.** Keratinocyte growth factor is an important endogenous mediator of hair follicle growth, development, and differentiation. *Am J Pathol* 147: 145–154, 1995.
9. **Davidson KG, Bersten AD, Barr HA, Dowling KD, Nicholas TE, and Doyle IR.** Lung function, permeability, and surfactant composition in oleic acid-induced acute lung injury in rats. *Am J Physiol Lung Cell Mol Physiol* 279: L1091–L1102, 2000.
10. **Derks CM and Jacobvitz-Derks D.** Embolic pneumopathy induced by oleic acid. *Am J Pathol* 87: 143–158, 1977.
11. **Dickey BF, Thrall RS, McCormick JR, and Ward PA.** Oleic-acid-induced lung injury in the rat. *Am J Pathol* 103: 376–383, 1981.
12. **Dreyfuss D, Soler P, Basset G, and Saumon G.** High inflation pressure pulmonary edema. *Am Rev Respir Dis* 137: 1159–1164, 1988.

13. **Dreyfuss D, Soler P, and Saumon G.** Mechanical ventilation-induced pulmonary edema. *Am J Respir Crit Care Med* 151: 1568–1575, 1995.
14. **Driscoll B.** Macrophage inflammatory proteins: biology and role in pulmonary inflammation. *Exp Lung Res* 20: 473–490, 1994.
15. **Eiermann GJ, Dickey BF, and Thrall RS.** Polymorphonuclear leukocyte participation in acute oleic-acid-induced lung injury. *Am Rev Respir Dis* 128: 845–850, 1983.
16. **Erjefält JS, Erjefält I, Sundler F, and Persson CGA.** In vivo restitution of airway epithelium. *Cell Tissue Res* 281: 305–316, 1995.
17. **Ewart S, Levitt R, and Mitzner W.** Respiratory system mechanics in mice measured by end-inflation occlusion. *J Appl Physiol* 79: 560–566, 1995.
18. **Fehrenbach H, Kasper M, Tschernig T, Pan T, Schuh D, Shannon JM, Mason RJ, and Mason RJ.** Keratinocyte growth factor-induced hyperplasia of rat alveolar type II cells in vivo is resolved by differentiation into type I cells and by apoptosis. *Eur Respir J* 14: 534–544, 1999.
19. **Finch PW, Rubin JS, Miki T, Ron D, and Aaronson SA.** Human KGF is FGF-related with properties of a paracrine effector of epithelial cell growth. *Science* 245: 752–755, 1989.
20. **Galiacy S, Planus E, Lepetit H, Féréol S, Laurent V, Ware LB, Isabey D, Matthay MA, Harf A, and d'Ortho MP.** Keratinocyte growth factor promotes cell motility during alveolar epithelial repair in vitro. *Exp Cell Res* 283: 215–229, 2003.
21. **Guery BP, Mason CM, Dobard EP, Beaucaire G, Summer WR, and Nelson S.** Keratinocyte growth factor increases transalveolar sodium reabsorption in normal and injured rat lungs. *Am J Respir Crit Care Med* 155: 1777–1784, 1997.
22. **Guo J, Yi ES, Havill AM, Sarosi I, Whitcomb L, Yin S, Middleton SC, Piguet P, and Ulich TR.** Intravenous keratinocyte growth factor protects against experimental pulmonary injury. *Am J Physiol Lung Cell Mol Physiol* 275: L800–L805, 1998.
23. **Hernandez LA, Coker PJ, May S, Thompson AL, and Parker JC.** Mechanical ventilation increases microvascular permeability in oleic acid-injured lungs. *J Appl Physiol* 69: 2057–2061, 1990.
24. **Hofman WF, Ehrhart IC, Granger WM, and Miller DA.** Sequential cardiopulmonary changes after oleic-acid injury in dogs. *Crit Care Med* 13: 22–27, 1985.
25. **Inoue S, Suzuki M, Nagashima Y, Suzuki S, Hashiba T, Tsuburai T, Ikehara K, Matsuse T, and Ishigatsubo Y.** Transfer of heme oxygenase 1 cDNA by a replication-deficient adenovirus enhances interleukin 10 production from alveolar macrophages that attenuates lipopolysaccharide-induced acute lung injury in mice. *Hum Gene Ther* 12: 967–979, 2001.
26. **Jefferies AL, Fung D, and Mullen JBM.** Fibrinogen depletion and control of permeability in oleic acid lung injury. *Am Rev Respir Dis* 143: 618–624, 1991.
27. **Jeffery PK and Corrin B.** Structural analysis of the respiratory tract. In: *Immunology of the Lung and the Upper Respiratory Tract*, edited by Bienenstock J. New York: McGraw-Hill, 1984, p. 1–27.
28. **Jeschke MG, Richter G, Höfstädter F, Herndon DN, Polo-Perez JR, and Jauch KW.** Non-viral liposomal keratinocyte growth factor (KGF) cDNA gene transfer improves dermal and epidermal regeneration through stimulation of epithelial and mesenchymal factors. *Gene Ther* 9: 1065–1074, 2002.
29. **Johanson WG, Holcomb JR, and Coalson JJ.** Experimental diffuse alveolar damage in baboons. *Am Rev Respir Dis* 126: 142–151, 1982.
30. **Kheradmand F, Folkesson HG, Shum L, Derynk R, Pytela R, and Matthay MA.** Transforming growth factor-α enhances alveolar epithelial cell repair in a new in vitro model. *Am J Physiol Lung Cell Mol Physiol* 267: L728–L738, 1994.
31. **Lee ER, Marshall J, Siegel CS, Jiang C, Yew NS, Nichols MR, Nietupski JB, Ziegler RJ, Lane MB, Wang KX, Wan NC, Scheule RK, Harris DJ, Smith AE, and Cheng SH.** Detailed analysis of structures and formulations of cationic lipids for efficient gene transfer to the lung. *Hum Gene Ther* 7: 1701–1717, 1996.
32. **Li S and Huang L.** In vivo gene transfer via intravenous administration of cationic lipid-protamine-DNA (LPD) complexes. *Gene Ther* 4: 891–900, 1997.
33. **Li S, Liu F, and Liu D.** Enhanced gene expression in mouse lung by prolonging the retension time of intravenously injected plasmid DNA. *Gene Ther* 5: 1531–1537, 1998.
34. **Li S, Wu SP, Whitmore M, Loeffert EJ, Wang L, Watkins SC, Pitt BR, and Huang L.** Effect of immune response on gene transfer to the lung via systemic administration of cationic lipidic vectors. *Am J Physiol Lung Cell Mol Physiol* 276: L796–L804, 1999.
35. **Marchese C, Chedid M, Dirsch OR, Csaky KG, Santanelli F, Latini C, LaRochelle WJ, Torrisi MR, and Aaronson SA.** Modulation of keratinocyte growth factor and its receptor in reepithelializing human skin. *J Exp Med* 182: 1369–1376, 1995.
36. **Mason CM, Guery BP, Summer WR, and Nelson S.** Keratinocyte growth factor attenuates lung leak induced by α-naphthylthiourea in rats. *Crit Care Med* 24: 925–931, 1996.
37. **Miki T, Fleming TP, Bottaro DP, Rubin JS, Ron D, and Aaronson SA.** Expression cDNA cloning of the KGF receptor by creation of a transforming autocrine loop. *Science* 251: 72–75, 1991.
38. **Minter RM, Ferry MA, Murday ME, Tannahill CL, Bahjat FR, Oberholzer C, Oberholzer A, LaFace D, Hutchins B, Wen S, Shinoda J, Copeland EM, and Moldawer LL.** Adenoviral delivery of human and viral IL-10 in murine sepsis. *J Immunol* 167: 1053–1059, 2001.
39. **Montaner JSG, Tsang J, Evans KG, Mullen JBM, Burns AR, Walker DC, Wiggs B, and Hogg JC.** Alveolar epithelial damage. *J Clin Invest* 77: 1786–1796, 1986.
40. **Moriuchi H, Zaha M, Fukumoto T, and Yuizono T.** Activation of polymorphonuclear leukocytes on oleic acid-induced lung injury. *Intensive Care Med* 24: 709–715, 1998.
41. **Morrison DF, Foss DL, and Murtaugh MP.** Interleukin-10 gene therapy-mediated amelioration of bacterial pneumonia. *Infect Immun* 30: 4752–4758, 2000.
42. **Mourgeon E, Isowa N, Keshavjee S, Zhang X, Slutsky AS, and Liu M.** Mechanical stretch stimulates macrophages inflammatory protein-2 secretion from fetal rat lung cells. *Am J Physiol Lung Cell Mol Physiol* 279: L699–L706, 2000.
43. **Nemzek JA, Ebong SJ, Kim J, Bolgos GL, and Remick DG.** Keratinocyte growth factor pretreatment is associated with decreased MIP-2α concentrations and reduced neutrophil recruitment in acid aspiration lung injury. *Shock* 18: 501–506, 2002.
44. **Oswari J, Matthay MA, and Margulies SS.** Keratinocyte growth factor reduces alveolar epithelial susceptibility to in vitro mechanical deformation. *Am J Physiol Lung Cell Mol Physiol* 281: L1068–L1077, 2001.
45. **Otterbein LE, Kolls JK, Mantell LL, Cook JL, Alam J, and Choi AMK.** Exogenous administration of heme oxygenase-1 by gene transfer provides protection against hyperoxia-induced lung injury. *J Clin Invest* 103: 1047–1054, 1999.
46. **Panos RJ, Bak PM, Simonet WS, Rubin JS, and Smith LJ.** Intratracheal instillation of keratinocyte growth factor decreases hyperoxia-induced mortality in rats. *J Clin Invest* 96: 2026–2033, 1995.
47. **Panos RJ, Rubin JS, Aaronson SA, and Mason RJ.** Keratinocyte growth factor and hepatocyte growth factor/scatter factor are heparin-binding growth factors for alveolar type II cells in fibroblast-conditioned medium. *J Clin Invest* 92: 977, 1993.
48. **Peterson GL.** A simplification of the protein assay methods of Lowry et al., which is more generally applicable. *Anal Biochem* 83: 346–356, 1977.
49. **Putnins EE, Firth JD, Lohachitranont A, Uitto VJ, and Larjava H.** Keratinocyte growth factor (KGF) promotes keratinocyte cell attachment and migration on collagen and fibronectin. *Cell Adhes Commun* 7: 211–221, 1999.
50. **Rosenthal C, Caronia C, Quinn C, Lugo N, and Sagy M.** A comparison among animal models of acute lung injury. *Crit Care Med* 26: 912–916, 1998.
51. **Schneeberger EE.** Alveolar type I cells. In: *The Lung*, edited by Crystal RG, West JB, Weibel ER, and Barnes PJ. Philadelphia, PA: Lippincott-Raven, 1997, p. 535–541.
52. **Schoene RB, Robertson HT, Thorning DR, Springmeyer SC, Hlastala MP, and Cheney FW.** Pathophysiological patterns of resolution from acute oleic acid lung injury in the dog. *J Appl Physiol* 56: 472–481, 1984.
53. **Schuster DP.** ARDS: clinical lessons from the oleic acid model of acute lung injury. *Am J Respir Crit Care Med* 149: 245–260, 1994.
54. **Simpson JA, Wallace WAH, Marsden ME, Govan JRW, Porteous DJ, Haslett C, and Sallenave JM.** Adenoviral augmentation of elafin protects the lung against acute injury mediated by activated neutrophils and bacterial infection. *J Immunol* 167: 1778–1786, 2001.
55. **Sugahara K, Iyama KI, Kuroda MJ, and Sano K.** Double intratracheal instillation of keratinocyte growth factor prevents bleomycin-induced lung fibrosis in rats. *J Pathol* 186: 90–98, 1998.
56. **Sun D, Zhao M, Ma D, Liao S, and Di C.** Protective effect of interleukin-1 receptor antagonist on oleic acid-induced lung injury. *Chin Med J* 109: 522–526, 1996.

57. **Sutherland LM, Edwards YS, and Murray AW.** Alveolar type II cell apoptosis. *Comp Biochem Physiol A* 129: 267–285, 2001.
58. **Syrbu S, Thrall RS, Wisniecki P, Lifchez S, and Smilowitz HM.** Increased immunoreactive rat lung ICAM-1 in oleic acid-induced lung injury. *Exp Lung Res* 21: 599–616, 1995.
59. **Takeoka M, Ward WF, Pollack H, Kamp DW, and Panos RJ.** KGF facilitates repair of radiation-induced DNA damage in alveolar epithelial cells. *Am J Physiol Lung Cell Mol Physiol* 272: L1174–L1180, 1997.
60. **Tan Y, Liu F, Li Z, Li S, and Huang L.** Sequential injection of cationic liposome and plasmid DNA effectively transfects the lung with minimal inflammatory toxicity. *Mol Ther* 3: 673–682, 2001.
61. **Tomashefski JF.** Pulmonary pathology of acute respiratory distress syndrome. *Clin Chest Med* 21: 435–465, 2000.
62. **Ulich TR, Yi ES, Cardiff R, Yin S, Bikhazi N, Biltz R, Morris CF, and Pierce GF.** Keratinocyte growth factor is a growth factor for mammary epithelium in vivo. *Am J Pathol* 144: 862–868, 1994.
63. **Ulich TR, Yi ES, Longmuir K, Yin S, Biltz R, Morris CF, Housley RM, and Pierce GF.** Keratinocyte growth factor is a growth factor for type II pneumocytes in vivo. *J Clin Invest* 93: 1298–1306, 1994.
64. **Veldhuizen RAW, Slutsky AS, Joseph M, and McCray PB.** Effects of mechanical ventilation of isolated mouse lungs on surfactant and inflammatory cytokines. *Eur Respir J* 17: 488–494, 2001.
65. **Viget N, Guery BP, Ader F, Alfandari S, Creuzy C, Roussel-Delvallez M, Foucher C, Mason CM, Beaucaire G, and Pittet JF.** Keratinocyte growth factor protects against *Pseudomonas aeruginosa*-induced lung injury. *Am J Physiol Lung Cell Mol Physiol* 279: L1199–L1209, 2000.
66. **Waters CM and Savla U.** Keratinocyte growth factor accelerates wound closure in airway epithelium during cyclic mechanical strain. *J Cell Physiol* 181: 424–432, 1999.
67. **Welsh DA, Summer WR, Dobard EP, Nelson S, and Mason CM.** Keratinocyte growth factor prevents ventilator-induced lung injury in an ex vivo rat model. *Am J Respir Crit Care Med* 162: 1081–1086, 2000.
68. **Wilson MR, Choudhury S, Goddard ME, O'Dea KP, Nicholson AG, and Takata M.** High tidal volume ventilation upregulates intrapulmonary cytokines in an in vivo mouse model of ventilator-induced lung injury. *J Appl Physiol* 95: 1385–1393, 2003.
69. **Wu KI, Pollack N, Panos RJ, Sporn PHS, and Kamp DW.** Keratinocyte growth factor promotes alveolar epithelial cell DNA repair after H_2O_2 exposure. *Am J Physiol Lung Cell Mol Physiol* 275: L780–L787, 1998.
70. **Yano T, Deterding RR, Nielsen LD, Jacoby C, Shannon JM, and Mason RJ.** Surfactant protein and CC-10 expression in acute lung injury and in response to keratinocyte growth factor. *Chest* 111: 137S–138S, 1997.
71. **Yano T, Deterding RR, Simonet WS, Shannon JM, and Mason RJ.** Keratinocyte growth factor reduces lung damage due to acid instillation in rats. *Am J Respir Cell Mol Biol* 15: 433–442, 1996.
72. **Yano T, Mason RJ, Pan T, Deterding RR, Nielsen LD, and Shannon JM.** KGF regulates pulmonary epithelial proliferation and surfactant protein gene expression in adult rat lung. *Am J Physiol Lung Cell Mol Physiol* 279: L1146–L1158, 2000.
73. **Yi ES, Salgado M, Williams S, Kim SJ, Masliah E, Yin S, and Ulich TR.** Keratinocyte growth factor decreases pulmonary edema, transforming growth factor-β and platelet-derived growth factor-BB expression, and alveolar type II cell loss in bleomycin-induced lung injury. *Inflammation* 22: 315–325, 1998.
74. **Yi ES, Williams ST, Lee H, Malicki DM, Chin EM, Yin S, Tarpley J, and Ulich TR.** Keratinocyte growth factor ameliorates radiation- and bleomycin-induced lung injury and mortality. *Am J Pathol* 149: 1963–1970, 1996.
75. **Yi ES, Yin S, Harclerode DL, Bedoya A, Bikhazi N, Housley RM, Aukerman SL, Morris CF, Pierce GF, and Ulich TR.** Keratinocyte growth factor induces pancreatic ductal epithelial proliferation. *Am J Pathol* 145: 80–85, 1994.
76. **Zahm JM, Kaplan H, Hérard AL, Doriot F, Pierrot D, Somelette P, and Puchelle E.** Cell migration and proliferation during the in vitro wound repair of the respiratory epithelium. *Cell Motil Cytoskeleton* 37: 33–43, 1997.
77. **Zhou MY, Lo SK, Bergenfeldt M, Tiruppathi C, Jaffe A, Xu N, and Malik AB.** In vivo expression of neutrophil inhibitory factor via gene transfer prevents lipopolysaccharide-induced lung neutrophil infiltration and injury by a β_2 integrin-dependent mechanism. *J Clin Invest* 101: 2427–2437, 1998.